REPORT ON CONSOLIDATION-INDUCED SOLUTE TRANSPORT

JANGGUEN LEE

ABSTRACT

Consolidation in cohesive soils mainly focuses on compressibility of soils, but it affects solute transport in some cases. The consolidation process takes on particular significance for fine grained soils at high water content, such as dredged sediments, but has also been shown to be important for compacted clay liners during waste filling operation. Numerical investigation using CST1 and CST2 was reviewed on consolidation-induced solute transport in this paper, especially with the development of CST2 model, verification by comparing experimental results with numerical simulations, and cases studies regarding transport in a confined disposal facility (CDF) and during in-situ capping. The importance of the consolidation process on solute transport is accessed based on simulated concentration or mass breakthrough curves. Results indicate that neglecting transient consolidation effects may lead to significant errors in transport analyses, especially with soft contaminated cohesive soils undergoing large volume change.

Key Words : Consolidation, Solute Transport, Sediments, CST1, CST2

1 INTRODUCTION

Solute transport has been widely studied for rigid porous media, but there are some cases where transport coupled with consolidation occurs. The consolidation process takes on particular significance for fine grained soils at high water content, such as dredged sediments, but has also been shown to be important for compacted clay liners during waste filling operations (Peter and Smith 2002; Alshawabkeh and Rahbar 2006; Fox 2007b). Transport processes are similar to those for rigid porous media and include advection, dispersion, and sorption/desorption effects, but consolidation involves transient advective flows that are governed by the dissipation of excess pore pressures and boundary drainage conditions. These flows produce volumetric strains that, in turn, cause changes in soil compressibility and hydraulic conductivity. As strains increase, changes in compressibility and hydraulic conductivity can become large and transport analyses are treated within the context of large strain consolidation theory (Gibson et al. 1995; Peter and Smith 2002; Fox 2007a).

Several key questions arise for any consolidation –induced solute transport cases (Fox 2007a): 1) What will be the amount and rate of pore water effluent? 2) What will be the concentration of contaminants in the effluent? 3) What will be the concentration and distribution of remaining contaminants in the dewatered sediments? Conventional solute transport models for rigid porous media are incapable of answering these questions because in this case advective flow is driven by the consolidation process.

Various numerical models have been developed to simulate solute transport within deforming porous media. In each case, the problem can be treated as semi-coupled, with transient advective flows driving the transport process but solute concentrations not affecting media consolidation. CST2 (Consolidation Solute Transport 2) based on the code CST1 (Fox 2007a) is the next level of sophistication beyond other models. This paper presents the results of a numerical investigation of the significance of consolidation on solute transport using CST1 and CST2.

2 COMPUTATIONAL MODEL

2.1 Description

CST2 is a computational model for coupled large strain consolidation and solute transport in saturated porous media (Fox and Lee 2008). The consolidation algorithm is one-dimensional and accounts for vertical strain, soil self-weight, general constitutive relations, relative velocity of fluid and solid phases, changing hydraulic conductivity and compressibility during consolidation, time-dependent loading, unload/reload effects and an external hydraulic gradient acting across the layer. Soil constitutive relationships are defined using discrete data points and can take nearly any desired form (Fig. 1). The solute transport algorithm of CST2 is two-dimensional and accounts for advection, longitudinal and transverse dispersion, changing effective diffusion coefficient during consolidation, first-order decay reactions and nonlinear nonequilibrium sorption. Solute transport is consistent with temporal and spatial variations of porosity and

Senior Researcher, Korea Institute of Construction Technology, South Korea.

seepage velocity in the consolidating layer.

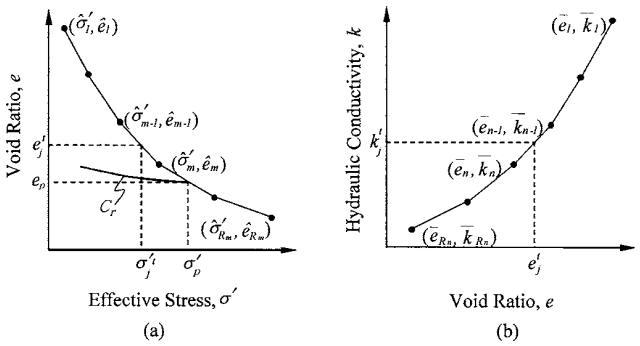

Figure 1. Soil constitutive relationships: (a) effective stress (σ') vs. void ratio (e), (b) hydraulic conductivity (k) vs. void ratio (e) (Fox et al. 2005)

The key to the transport model is the definition of two Lagrangian fields of elements that follow the motions of fluid and solid phases separately (Fig. 2). This reduces numerical dispersion and simplifies transport calculations to that of dispersion mass flow between contiguous fluid elements (Fox 2007a).

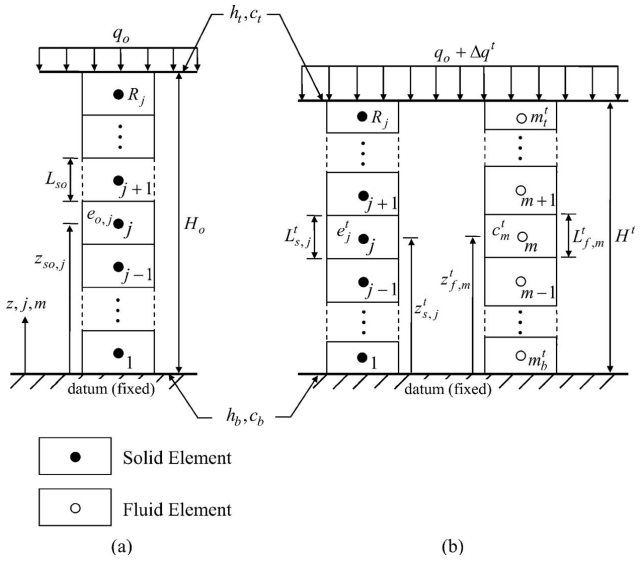

Figure 2. Geometry for CST2: (a) initial configuration; (b) after application of stress increment (Fox and Lee 2008)

2.2 Verification

Verification checks of CST1 and CST2 show excellent agreement with analytical and numerical solutions for solute transport in rigid and compressible porous media (Fox 2007b; Fox and Lee 2008). Further experimental and numerical results were used to evaluate model validity.

A tested specimen was prepared with kaolinite clay and potassium bromide (KBr) solution. The material is classified as lean clay (CL) with a specific gravity (G_s) = 2.61, liquid limit (LL) = 47.6, and plastic limit (PI) = 21.8. The solute transport test was conducted on a composite kaolinite specimen with an upper uncontaminated layer prepared with de-ionized water and a lower contaminated slurry layer with target concentration of 1635 mg/L Br^- and 800 mg/L K^+. The target initial water content for each layer was 2 LL . The experimental apparatus used in the investigation is shown in Fig. 3. Contaminated and uncontaminated slurry layers were placed in a rigid wall consolidation cell (dia. = 102 mm) by a combination of spooning and pouring. Care was taken during this process to entrain as little air as possible into the slurry and thus maintain a saturated condition. Filter paper was placed adjacent to porous discs at the top and bottom of the specimen and in between the slurry layers to provide separation. Table 1 provides the initial layer heights, initial void ratios (e_o), and initial pore fluid concentrations (c_o) for the lower layer of the test specimen. Initial potassium concentration in the contaminated kaolinite layer is well below the standard solution concentration (800 mg/L) due to potassium sorption onto the solid phase. Each test began immediately after the composite specimen was prepared to minimize diffusion transport into the upper uncontaminated layer prior to testing.

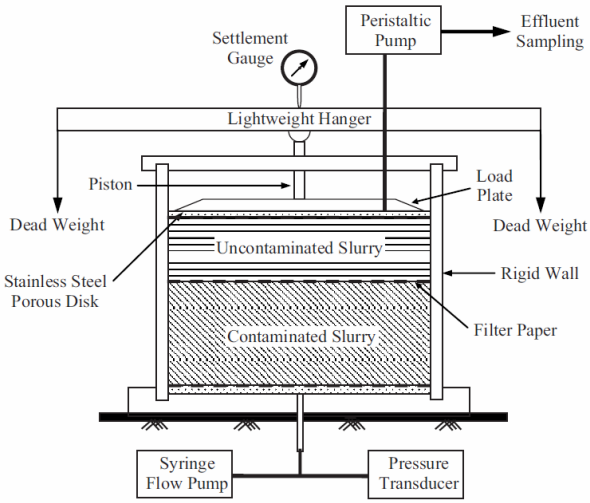

Figure 3. Consolidation test apparatus and composite kaolinite specimen (Lee and Fox 2009b)

Table 1. Initial condition of solute transport test

Uncontaminated Layer (top)		Contaminated Layer (bottom)			
Height (mm)	e_o	Height (mm)	e_o	Br^- c_o (ppm)	K^+ c_o (ppm)
21.1	2.51	50.6	2.46	1677	270.4

The consolidation-induced solute transport test was conducted with single-drained at the top boundary with pore pressure measurements taken at the base. Thus, advection occurred upward from the contaminated

slurry layer and through the uncontaminated slurry layer. A zero concentration gradient was maintained at both boundaries. This condition was achieved at the top boundary by continuously removing all pore water effluent using a peristaltic pump. The inflow line to the pump was inserted through a hole in the load plate such that it could collect pore fluid at the top boundary as soon as it was expelled into the stainless steel porous disk. The loading schedule consisted of six increments (3.1, 5.6, 10.4, 20.1, 39.5, 78.4 kPa). Each load increment remained on the specimens for 3 days, with primary consolidation generally finished in approximately 2 days. Therefore, the total testing period was 18 days. Dial gage readings taken after primary consolidation indicated that there was insignificant secondary compression for this soil.

An independent series of batch, diffusion, dispersion, and consolidation tests were performed to obtain input parameters for the CST2 computational model (Lee and Fox 2009a). The compressibility relationship was obtained from the final void ratio at each load increment and the hydraulic conductivity was defined by $e = 8.16 + 0.765 \log k$, where k is the vertical hydraulic conductivity (m/s). The effective diffusion coefficient was defined as $D^* = (n)^M D_o$, where D_o is the free solution diffusion coefficient (2.08×10^{-9} m^2/s for Br- and 1.96×10^{-9} m^2/s for K+), n is porosity, and $M = 1.84$. Values of dispersivity (α_L) showed no clear trend with decreasing void ratio and yielded averages of $\alpha_L = 0$ and $\alpha_L = 20$ mm for Br^- and K^+, respectively. Mechanical dispersion was therefore not included for the Br^- simulations. The nonequilibrium sorption isotherm for K^+ was defined as $\partial s/\partial t = \lambda(K_P c^F - s)$, where s is the sorbed concentration, t is time, $\lambda = 0.005$/s, $K_P = 19.6$ mL/g, and $F = 0.608$. The soil specimen was modeled as single-drained on top with zero concentration gradient at both boundaries and using a total of 200 solid elements and 600 fluid elements.

Measured and computed settlement curves are presented in Fig. 4. Final settlement corresponds to average vertical strain of 37%, and indicates that very large strain was achieved in the test. Simulated settlement result is very close to the measured data, which corroborates the ability of CST2 to model large strain consolidation. Solute effluent concentrations are also presented in Fig. 4. Effluent concentration curve for Br^- shows increasing concentrations in the pore water effluent with increasing settlement. This occurs because larger settlements correspond to greater advective transport from the contaminated kaolinite layer into the uncontaminated kaolinite layer. Corresponding curve for K^+ indicates much smaller effluent concentrations because potassium was sorbed to the uncontaminated layer during upward transport and less was carried out of the specimen. The CST2 simulations are in good agreement with Br^- and K^+ effluent concentrations for both tests.

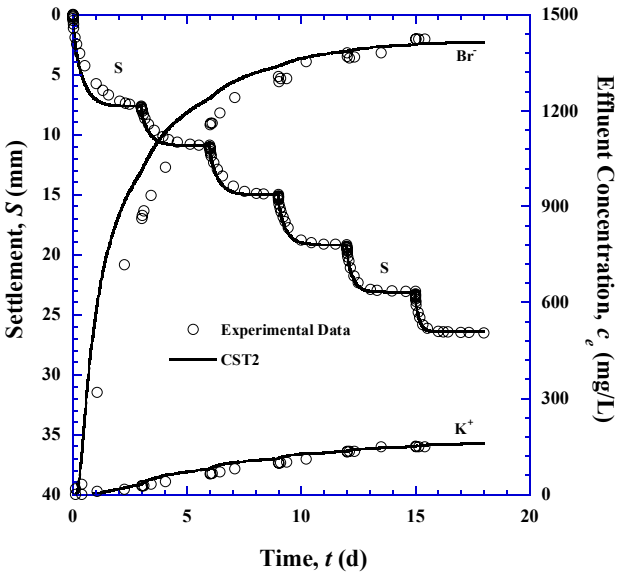

Figure 4. Measured and simulated settlement and breakthrough curves

3 Case Studies

3.1 Confined Disposal Facility

The results of case studies using CST1 and CST2 are now presented to show the significance of consolidation on solute transport. First, CST1 is used to simulate consolidation-induced solute transport when dredged contaminated sediments are impounded in a confined disposal facility (CDF). Readers can find more detail information from previous work (Fox 2007b), and herein only presents summary of it.

The geometry is shown in Fig. 5. The bottom of the CDF is lined and may contain a leachate collection system (LCS). Saturated sediment slurry is placed relatively quickly to an initial height of 8 m and then consolidates by self-weight. The slurry contains tetrachloroethene (PCE) and polychlorinated biphenyls (PCBs), and simulation assumes that both PCE and PCB have a uniform initial concentration of $c_o = 100$ mg/L in a layer of slurry between elevations $z = 6$m to 7m (Fig. 5). The remainder of the slurry mass is initially uncontaminated. The top boundary is drained and maintained at zero concentration (Type I). The bottom boundary may be drained or undrained, depending on the presence of the LCS. If drained, it is assumed the LCS is at atmospheric pressure and creates a zero concentration gradient (Type II) boundary. If undrained, the liner constitutes a no-flow boundary for both water and contaminants.

The top concentration boundary is kept as zero concentration, so it is not useful to present simulated breakthrough curves with respect to concentration. On

the other hand, contaminant mass outflows per unit area are presented in Fig. 6 and they clearly show that contaminant mass outflows are strongly influenced by consolidation-induced advection.

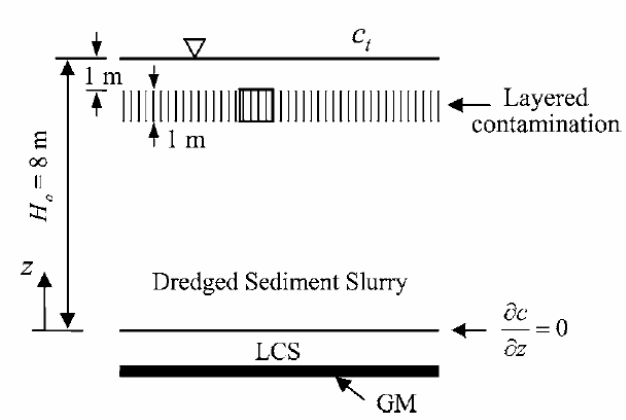

Figure. 5. Initial geometry for dredged sediment slurry in a confined disposal facility (Fox 2007b)

Outflows are largest for the single-drained (SD) case because all fluid is discharged at the top boundary. When the layer is double-drained (DD), smaller mass outflows are calculated for a 50 yr period because some of the contaminants move downward toward the more distance bottom boundary. The larger distribution coefficient for PCB renders it much less mobile than PCE and consequently results in significantly smaller mass outflows. Fifty years after placement, the percentage of initial PCE mass that leaves the system is 19% for no consolidation (NC), 72% for SD, and 36% for DD. Corresponding values for PCB are 0.3, 2.5, and 1.3%.

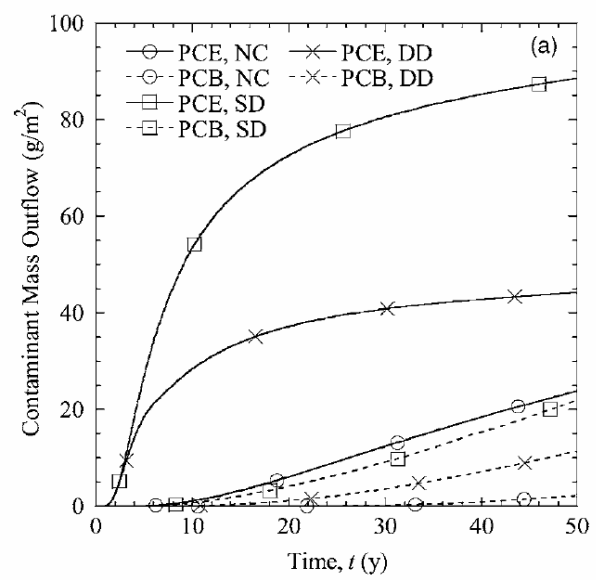

Figure. 6. Contaminant mass outflows in CDF with layered initial contamination (Fox 2007b)

3.2 In-Situ Capping

As a final example, CST2 is used to simulate the consolidation-induced transport when in-situ capping is applied to isolate contaminants at the bottom of river. The geometry of in-situ capping is shown in Fig. 7. Contaminated sediments have been accumulated over residual uncontaminated sediments, and in-situ capping overlies the contaminated sediments. A composite layer with 3m of initial height (H_o) consists of 1.5m of a bottom uncontaminated, 0.5m of a middle contaminated, and 1.0m of a top capping layer. Materials for all layers are assumed to be the same, and have a specific gravity of sediments (G_s)=2.70 and initial void ratio (e_o)=1.40. α_L was assumed to be zero, so D_h is equal to D^* which was assumed to be 5×10^{-10} m^2/s and constant during consolidation. Initial contaminant concentration is 100mg/L in the contaminated layer, and sorption isotherm is linear equilibrium with distribution coefficient (K_d) = 15mL/g in both the contaminated and uncontaminated layers. There is no chemical reaction in the capping layer (i.e., K_d = 0mL/g). Fig. 7(b) presents that groundwater flows upward direction with initial boundary hydraulic head of top (h_{wt}) and bottom (h_{wb}) are 8.5m and 10.0m, respectively. The composite layer was modeled using a total of 150 solid elements and 450 initial fluid elements. All simulations correspond to one-dimensional advection and transport with double-drained boundary condition and zero constant concentration at both top (c_t) and bottom (c_b) composite layer boundaries.

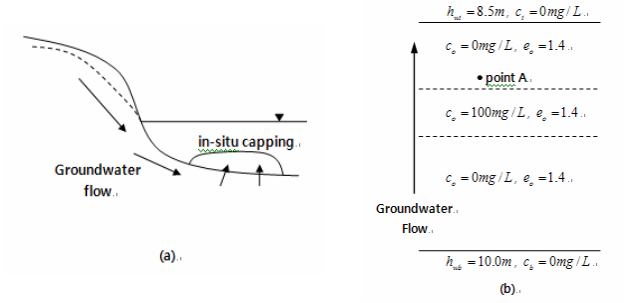

Figure. 7. Geometry of in-situ capping with a groundwater flow condition: (a) conceptual illustration of in-situ capping, and (b) geometry for 1D contaminant transport

Sediments initially possess high moisture content, so small surcharge load causes large strain consolidation. In order to simulate large strain consolidation, established constitutive relationships such as void ratio (e) vs. effective stress (σ') and void ratio (e) vs. hydraulic conductivity (k) are required as follow:

$$e = -0.21\log(\sigma') + 1.142 \qquad \text{(kPa)} \qquad (1)$$

$$e = 0.38\log(k) + 4.095 \quad \text{(m/s)} \qquad (2)$$

Eq (1) and (2) were taken from Grand Calumet River sediments in Gary, Indiana.

Fig. 8(a) presents changing height (H) as a function of time (t). Case I is considered when consolidation is ignored, but Case II presents consolidation-induced transport. For Case I, height keeps constant. However, for Case II, height decreases because self-weight of the composite layer causes consolidation. Final height is 2.54m, and volumetric strain becomes 15.5% with which large strain consolidation (>10%) is achieved. Consolidation is completed after t = 3.6yr.

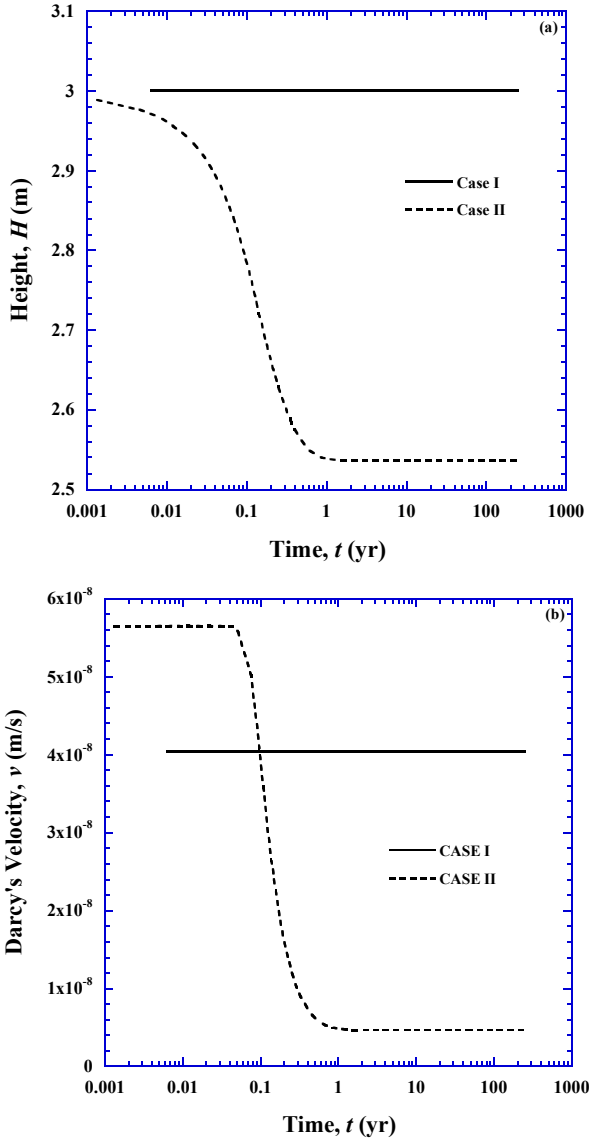

Figure. 8. Numerical simulations with consolidation (Case I) and without consolidation (Case II): (a) settlement and (b) discharge velocity at point A

Consolidation and groundwater flow take on particular significance in contaminant transport because they are directly related to advective process. In order to see changing discharge velocity (v) as a function of time, observation point (A, Fig. 7b) is located at 100mm above the contaminated layer and simulated discharge velocities for both Case I and II are presented in Fig. 8(b). For Case I, the discharge velocity of groundwater flow, following Darcy's law ($v = ki$) and using Eq (2), is constantly 4.04×10^{-8} m/s, where i is hydraulic gradient (($h_{wb} - h_{wt}$)/ H_o =1.5/3.0 = 0.5). The discharge velocity for Case II is various during consolidation due to changing hydraulic conductivity, hydraulic head in the composite layer caused by excess pore pressure, and height of the composite layer. Finally, after 100% consolidation, hydraulic conductivity and hydraulic gradient are different from the initial condition. As shown in Fig 8(b), final discharge velocity ($v = 4.60\times10^{-9}$ m/s) at point A is approximately 10 times less for Case II than for Case I.

Measured contaminant breakthrough curves at the point A are presented in Fig. 9 with logarithmic time scale. Contaminant concentration increases more quickly for Case II than Case I. This results from consolidation because discharge velocity of point A in Fig. 8(b) is faster for Case II than Case I until consolidation proceeds to 45.6% (t =36.5d=0.1yr). On the other hand, contaminant concentration decreases more slowly for Case II than Case I because discharge velocity is significantly reduced after consolidation.

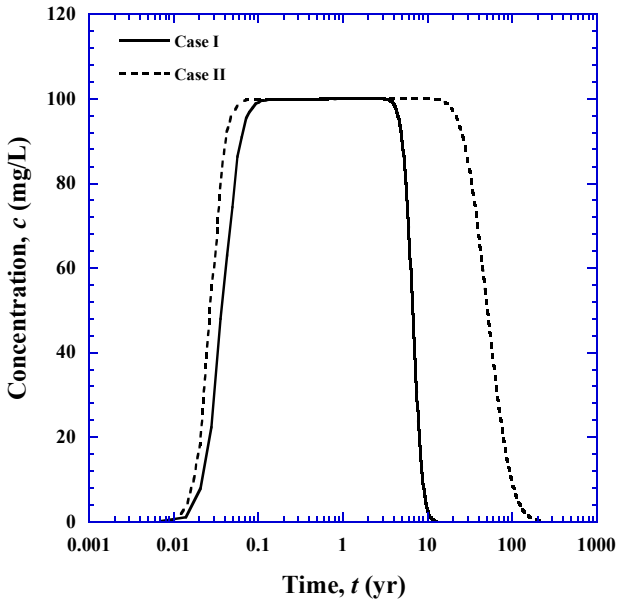

Figure. 9. Simulated breakthrough curves through point A on semilog plot with consolidation (Case I) and without consolidation (Case II)

4 CONCLUSION

The following conclusions are based on numerical simulations with CST1 and CST2 performed to investigate the consolidation-induced solute transport.

1. Numerical simulations obtained using the CST2 model were in good to excellent agreement with all experimental measurements. Comparisons were made based on settlement and solute breakthrough. This suggests that the CST2 computational model is capable of simulating local flow and transport effects for consolidation-induced transport of both tracer and reactive contaminant species.
2. Consolidation plays an important role on contaminant transport. This limited study has indicated that neglecting to consider transient consolidation effects may lead to serious errors in transport analyses for soft contaminated clays undergoing large strain consolidation.
3. Conventional capping installation with non-reactive materials significantly accelerates dissolved contaminant release during consolidation, and long-term release with high concentration occurs after consolidation.

ACKNOWLEDGEMENT

The author gratefully acknowledges financial support for this investigation provided in part by in-situ capping on contaminated sediment research from Korea Institute of Construction and Technology (KICT).

REFERENCES

1) Alshawabkeh, A. N., and Rahbar, N. (2006), "Parametric study of one-dimensional solute transport in deformable porous media." *Journal of Geotechnical and Geoenvironmental Engeering*, Vol. 132, No, 8, 1001-1010.
2) Fox, P. J. (2007a), "Coupled large strain consolidation and solute transport. I: Model development." *J. Geotech. Geoenviron. Eng.*, Vo. 133, No. 1, pp.3–15.
3) Fox, P. J. (2007b), "Coupled large strain consolidation and solute transport II: Model verification and simulation results." *Jounral of Geotechnical and Geoenvironmental Engineering*, Vol. 133, No. 1, 16-29.
4) Fox, P. J., Lee, J. and Qiu, T. (2005). "Model for large strain consolidation by centrifuge," *International Journal of Geomechanics*, ASCE, Vol. 5, No. 4, 267-275.
5) Fox, P. J., and Lee, J. (2008), "Model for consolidation-induced solute transport with nonlinear and nonequilibrium sorption," *International Journal of Geomechanics*, Vol. 8, No. 3, pp.188-198.
6) Gibson, R. E., Potter, L. J., Savvidou, C., and Schiffman, R. L. (1995). "Some aspects of one-dimensional consolidation and contaminant transport in wastes," *Proceedings, International Symposium on Compression and Consolidation of Clayey Soils*, H. Yoshikuni and O. Kusakabe, eds., Hiroshima, Japan, 2, pp. 815-845.
7) Lee, J., Fox, P. J., and Lenhart, J. J. (2009a), "Investigation of consolidation-induced solute transport. I: Effect of consolidation on transport parameters," *Journal of Geotechnical and Geoenvironmental Engineering*, Vol. 135, No. 9, pp.1228-1238.
8) Lee, J., and Fox, P. J. (2009b), "Investigation of consolidation-induced solute transport. II: Experimental and numerical results," *Journal of Geotechnical and Geoenvironmental Engineering*, Vol. 135, No. 9, pp.1239-1253.
9) Peters, G. P. and Smith, D. W. (2002). "Solute transport through a deforming porous medium," *International Journal for Numerical and Analytical Methods in Geomechanics*, 26(7), pp. 683-717.